AIAA SciTech
4-8 January 2016, San Diego, California, USA
54th AIAA Aerospace Sciences Meeting

Domain Decomposition in POD-Galerkin Projection for Flows with Moving Boundary

Haotian Gao*, Mingjun Wei†
New Mexico State University, Las Cruces, NM 88003

In this paper, we extended the application of POD-Galerkin projection for model order reduction from usual fixed-domain problems to more general fluid-solid systems when moving boundary/interface is involved. The idea is similar to numerical simulation approaches using embedded force terms to represent boundary motion and domain change. The embedded boundary allows a globally defined fixed domain including both fluid and solid, where POD-Galerkin projection can be directly applied. However, such a modified approach will not get away with the unsteadiness of boundary terms which appear as time-dependent coefficients in the new Galerkin model. These coefficients need to be precomputed for prescribed periodic motion, or worse, to be computed at each time step for non-prescribed (e.g. with fluid-structure interaction) or non-periodic situation. Though the time cost of computing these unsteady coefficients is smaller, as the associated integration is only in the close neighborhood of moving boundaries, it is still much higher than typical Galerkin model with constant coefficients. The extra computational cost gets expensive in some cases and eventually undermines the value of using reduced-order models. The further study shows, however, that the most expensive integration resulted from the unsteady motion has almost negligible impact on the overall dynamics. Dropping these expensive terms reduces the computation cost by at least one order while no obvious effect on model accuracy is noticed. A more aggressive approach is to decompose the moving boundary/domain to orthogonal modes and derive another low-order model with fixed coefficients for boundary motion. With domain decomposition, we have two coupled low-order models both with fixed coefficients and therefore the combined model is fast. Though the model with domain decomposition is less accurate at the boundary, it seems a fair trade-off for its benefit on computational cost saving.

I. Introduction

High-fidelity large-scale numerical simulation has been one of the most important research tools for the understanding of fluid dynamics, structural dynamics, fluid-structure interaction, and other problems in a broad scientific community. While the numerical simulation is getting more capable with the advances in computers and computational science, the computational cost of high-fidelity simulation is still too high to be practical in situations such as real-time control and fast optimal design. Reduced-order models (ROM) provide a way for fast computation with reasonable accuracy. One way to construct ROM is to use a "top-down" approach, which starts with a complete first-principle model (i.e. the one used by high-fidelity simulation) and reduces its cost by mapping the problem to a low-order space. The "top-down" approach is often called model (order) reduction to denote its difference from other "bottom-up" approaches (e.g. phenomenological model) for ROM.

Since its introduction to fluid mechanics community [1, 2], proper orthogonal decomposition (POD)-Galerkin projection has quickly become a popular tool for model reduction. POD-Galerkin projection has been successfully applied to solve many fluid problems [3–13]. However, most early studies are limited for fluid flows in a fixed or infinite domain. The implementation of traditional POD-Galerkin projection is not straightforward when there is a moving solid boundary or structure in fluid flow, which is the case in many modern applications including flapping-wing micro air vehicles, robot fish, energy harvesters, and wind

*Research Assistant, Department of Mechanical and Aerospace Engineering
†Associate Professor, Department of Mechanical and Aerospace Engineering, Associate Fellow AIAA

turbines. As it is reviewed recently [14], actuation modes [15, 16] and Eulerian-Lagrangian dynamic mesh adaptation methods [17–20] have been proposed to allow the transition between the moving/deforming near field to the stationary far field. There was also a different route taken by Liberge and Hamdouni, where they considered a fictitious stationary domain including both fluid and solid and applied POD-Galerkin projection on a modified equation for both fluid and solid [21]. Their approach shares some similarity with our earlier effort [22, 23] and more complete work presented in this paper, where we also considered both fluid and solid in a combined stationary domain. The idea was borrowed from immersed boundary technique used in numerical simulation [24–26], where the effect of moving boundary is represented as extra bodyforce terms added to the original Navier-Stokes equation, and then develop a global POD-Galerkin projection in a fixed domain with moving bodyforce terms for boundaries. Different from the approach of Liberge and Hamdouni [21], our method allows large and arbitrary movement of boundaries though only prescribed motion is considered at this moment. The difference between the current paper and our earlier work lies in the description of solid motion, which was a continuous domain with prescribed motion earlier [23] and a combination of decoupled modes with time-dependent coefficients currently. Further study of time cost on individual terms also allows us to drop the most expensive term without noticeable change to the results in current study.

For the rest of the paper, the basic methodology is introduced in §II, then the method is applied respectively to a flow passing a two-dimensional oscillatory cylinder and a three-dimensional oscillatory sphere in §III. The analysis of individual time cost and the discussion on the effect from dropping the most expensive term are in §IV. Finally, the conclusion is in §V.

II. Methodology

In this section, for completeness and clarity, we first have a quick review of the traditional POD-Galerkin projection for Navier-Stokes equation [2,3] and our earlier approach for global POD-Galerkin projection with moving solid domain [23]. Then, a new global approach with solid domain decomposition is introduced.

II.A. Traditional POD-Galerkin projection for fluid flows

Proper orthogonal decomposition (POD) was proved an efficient way of capturing the dominant components of an infinite-dimensional process with finite and often only a few number of modes [2]. The idea of Galerkin projection is to project the functions defining the original equation onto a finite-dimensional subspace of the full phase space [2]. To perform Galerkin projection, the phase space $\mathcal{X}$ must be an inner product space spanned by a suitable set of basis functions. The suitable choices for basis functions include *mathematical modes*, such as Fourier modes and Chebyshev polynomials, as well as *empirical modes*, such as POD modes.

Using POD together with Galerkin projection, we have a systematic procedure to obtain ROMs from simulation or experimental data. For traditional fluid mechanics problems, the approach can be applied on Navier-Stokes equation [2, 3]:

$$\frac{\partial \mathbf{u}}{\partial t} + \mathbf{u} \cdot \nabla \mathbf{u} = -\nabla p + \frac{1}{\mathrm{Re}} \nabla^2 \mathbf{u}, \tag{1}$$

where $\mathbf{u}$ is the velocity vector, p is the pressure, and Re is the Reynolds number. The velocity can be expanded about its mean value $\mathbf{u}_0$ and on POD modes $\boldsymbol{\phi}_j$ as

$$\mathbf{u} \approx \mathbf{u}^N = \mathbf{u}_0 + \sum_{j=1}^{N} a_j(t) \boldsymbol{\phi}_j(\mathbf{x}), \tag{2}$$

where the finite truncation at $j = N$ is performed for low-dimensional modeling. Substitite (2) in (1) and project the equation one to bases $\boldsymbol{\phi}_i$ to get dynamic equations for time coefficients,

$$\dot{a}_i = \frac{1}{\mathrm{Re}} \sum_{j=0}^{N} l_{ij} a_j + \sum_{j=0}^{N} \sum_{k=0}^{N} q_{ijk} a_j a_k, \qquad i = 1, ..., N, \tag{3}$$

where $l_{ij} = \langle \nabla^2 \boldsymbol{\phi}_j, \boldsymbol{\phi}_i \rangle_\Omega$ and $q_{ijk} = \langle \nabla \cdot (\boldsymbol{\phi}_j \boldsymbol{\phi}_k), \boldsymbol{\phi}_i \rangle_\Omega$. $\boldsymbol{\phi}_0 = \mathbf{u}_0$ and $a_0 = 1$ are introduced here for simple notation. In (3), orthogonality has been applied and the pressure term has been cancelled by appropriate boundary conditions (e.g. periodic condition).

II.B. Global POD-Galerkin projection for flows with moving boundary: continuous approach

The traditional approach of POD-Galerkin projection requires fixed fluid domain, which is not the case for flows with moving solid boundaries and structures. Instead of considering a time-dependent fluid domain, in an earlier study [23], we treated the combination of fluid and solid as one whole stationary domain. The idea is similar to immersed boundary technique used in numerical simulation [24–26], where the combined domain allows simple fixed meshes for discretization and the effect of moving boundary/structure is represented as extra body-force terms added to the original Navier-Stokes equation on specific "solid" area. Here, it is similar to immersed boundary method that the global Galerkin projection is based on a modified Navier-Stokes equation for the combined domain [27–29]:

$$\frac{\partial \mathbf{u}}{\partial t} + \mathbf{u} \cdot \nabla \mathbf{u} = -\nabla p + \frac{1}{\mathrm{Re}} \nabla^2 \mathbf{u} + \mathbf{f}, \tag{4}$$

where $\mathbf{f}$ is an extra bodyforce term added in solid domain Ω_s to define the trajectory of solid boundary/structure:

$$\mathbf{f} = \begin{cases} (\mathbf{u} \cdot \nabla \mathbf{u} - \frac{1}{\mathrm{Re}} \nabla^2 \mathbf{u})^n + \frac{1}{\triangle t}(\mathbf{V} - \mathbf{u}^n) & in \quad \Omega_s \\ 0 & otherwise \end{cases}, \tag{5}$$

with $\mathbf{V}$ being the prescribed velocity of solid, the pressure term has been neglected.

With the modified fluid-solid equation (4), the classical approach for fixed fluid domain can be directly applied on the whole fluid-solid domain to get

$$\dot{a}_i = \sum_{j=0}^{N} (\frac{1}{\mathrm{Re}} l_{ij} - l'_{ij}) a_j - \sum_{j=0}^{N} \sum_{k=0}^{N} (q_{ijk} - q'_{ijk}) a_j a_k + c'_i, \qquad i = 1, ..., N, \tag{6}$$

which is similar to the traditional form in (3). However, the new dynamic equation (6) has some new parameters defined by inner products with support only in solid domain:

$$l'_{ij} = \langle (\frac{1}{Re} \nabla^2 \boldsymbol{\phi}_j + \frac{1}{\Delta t} \boldsymbol{\phi}_j), \boldsymbol{\phi}_i \rangle_{\Omega_s(t)}, \tag{7}$$

$$q'_{ijk} = \langle \nabla \cdot (\boldsymbol{\phi}_j \boldsymbol{\phi}_k), \boldsymbol{\phi}_i \rangle_{\Omega_s(t)}, \tag{8}$$

$$c'_i = \langle \frac{1}{\Delta t} \mathbf{V}^n, \boldsymbol{\phi}_i \rangle_{\Omega_s(t)}, \tag{9}$$

and old parameters with similar definition but being extended to with support in the entire combined domain with both fluid and solid. It is worth noting that the corresponding global POD modes are also defined by inner products in the combined fluid-solid domain without telling difference between fluid and solid. For simplicity, we keep the same weight for the energy contribution from fluid and solid area in the definition of inner product, however, it is possible to consider fluid and solid with different weight and the change may improve the global POD modes for better ROM performance. The resulted model (6) describes globally both fluid and solid. Different from the approach by Liberge and Hamdouni [21], this approach allows large and arbitrary movement of boundaries though only prescribed motion is considered at this moment.

II.C. Global POD-Galerkin projection for flows with moving boundary: discrete domain-decomposition approach

In above derivation, since the solid domain $\Omega_s(t)$ is a time-dependent function, the integration in (7–9) needs to be computed at every time step. Though the computational process for simple integration is much less complex than the original high-fidelity model and the solid domain and its close neighborhood is also much smaller than the fluid domain, the increased computational cost by these terms are much larger than the ROM itself and overshadows the merit of using ROM. In the current work, solid domain decomposition [21] is implemented to remove this extra cost.

Introducing a characteristic function,

$$\chi_s = \begin{cases} 1 & in \quad \Omega_s \\ 0 & otherwise \end{cases}, \tag{10}$$

the integration in (7–9) can be rewritten as:

$$l'_{ij} = \langle (\frac{1}{Re}\nabla^2 \boldsymbol{\phi}_j + \frac{1}{\Delta t}\boldsymbol{\phi}_j), \chi_s \boldsymbol{\phi}_i \rangle, \tag{11}$$

$$q'_{ijk} = \langle \nabla \cdot (\boldsymbol{\phi}_j \boldsymbol{\phi}_k), \chi_s \boldsymbol{\phi}_i \rangle, \tag{12}$$

$$c'_i = \langle \frac{1}{\Delta t}\mathbf{V}^n, \chi_s \boldsymbol{\phi}_i \rangle. \tag{13}$$

Similar to the fluid field, the solid domain itself, marked now by χ, can also be decomposed to individual modes and the dimension is then reduced from a continuous space (or a space at the order of grid points in numerical simulation) to a low-order space with a truncated number of modes:

$$\chi_s(x,t) = \sum_{m=0}^{\infty} b_m(t)\psi_m(x) \approx \sum_{m=1}^{M} b_m(t)\psi_m(x), \tag{14}$$

where ψ is the solid modes computed by a similar POD approach but applied on domain function χ. The truncation of modes provides a good approximation of the same coefficients:

$$l'_{ij} \approx \sum_{m=0}^{M} \langle (\frac{1}{Re}\nabla^2 \boldsymbol{\phi}_j + \frac{1}{\Delta t}\boldsymbol{\phi}_j), \psi_m \boldsymbol{\phi}_i \rangle b_m = \sum_{m=0}^{M} l^*_{ijm} b_m, \tag{15}$$

$$q'_{ijk} \approx \sum_{m=0}^{M} \langle \nabla \cdot (\boldsymbol{\phi}_j \boldsymbol{\phi}_k), \psi_m \boldsymbol{\phi}_i \rangle b_m = \sum_{m=0}^{M} q^*_{ijkm} b_m, \tag{16}$$

$$c'_i \approx \sum_{m=0}^{M} \langle \frac{1}{\Delta t}\mathbf{V}^n, \psi_m \boldsymbol{\phi}_i \rangle b_m = \sum_{m=0}^{M} c^*_{im} b_m, \tag{17}$$

where the new integrals, l^*_{ijm}, q^*_{ijkm}, and c^*_{im}, are not time-dependent and need to compute only once for each mode. The time-dependent components are coefficients b_m's now which have much lower order (i.e. number of domain modes) compared to the order of the original solid domain (i.e. number of mesh points in solid domain). Put these new terms in equation (6), the model becomes:

$$\dot{a}_i = \sum_{j=0}^{N} (\frac{1}{\mathrm{Re}} l_{ij} - \sum_{m=0}^{M} l^*_{ijm} b_m) a_j - \sum_{j=0}^{N}\sum_{k=0}^{N} (q_{ijk} - \sum_{m=0}^{M} q^*_{ijkm} b_m) a_j a_k + \sum_{m=0}^{M} c^*_{im} b_m, \qquad i = 1, ..., N. \tag{18}$$

To close the system, a level-set like equation is introduced to track the domain change [21] :

$$\dot{b}_n = -\sum_{n=0}^{N} \langle \boldsymbol{V}(x,t) \cdot \nabla \boldsymbol{\psi}_m, \psi_n \rangle b_m, \qquad n = 1, ..., N. \tag{19}$$

For simple motions such as the one-dimensional oscillation used in this paper, the integration is simplified to

$$\langle \boldsymbol{V}(x,t) \cdot \nabla \boldsymbol{\psi}_m, \psi_n \rangle = V(t) \langle \vec{n}_y \cdot \nabla \boldsymbol{\psi}_m, \psi_n \rangle, \tag{20}$$

and the domain morphing is then

$$\dot{b}_n = -V(t) \sum_{n=0}^{N} K_{mn} b_m, \qquad n = 1, ..., N, \tag{21}$$

with the prescribed oscillation velocity $V(t)$ given and the fixed coefficients K_{mn} computed by

$$K_{mn} = \langle \vec{n}_y \cdot \nabla \boldsymbol{\psi}_m, \psi_n \rangle. \tag{22}$$

III. Applications on 2D and 3D flows

The proposed method is first applied on a two-dimensional flow passing an oscillatory cylinder and then on a three-dimensional flow passing an oscillatory sphere.

III.A. Two-dimensional flow passing an oscillatory cylinder

Figure 1. A schematic of flow passing an oscillatory cylinder.

As sketched in figure 1, a two-dimensional cylinder oscillates (along y) normal to the incoming flow. The Reynolds number is 100, which is defined by the incoming velocity and cylinder diameter. The computational domain is $l_x \times l_y = (0, 50) \times (0, 30)$ with uniform mesh at $N_x \times N_y = 1000 \times 600$, and the neutral position of the cylinder center is at $(x_0, y_0) = (10, 15)$. The oscillation is defined by $y(t) = y_0 + A\sin(2\pi ft)$ with amplitude $A = 1.5$ and frequency $f = 0.2$. Here, the large amplitude is picked intentionally to challenge the capability of our approach to handle large domain change. The numerical algorithm is the same as the one reported and tested in our previous numerical simulations [28, 29], where the projection method is applied to solve incompressible Navier-Stokes equations [30], the 3rd-order Runge-Kutta method is used for time advancement, and the immersed boundary method is implemented to describe moving boundaries/structures [26].

With the chosen amplitude and frequency, the wake vortex structure from our simulation shows complicated P+S pattern (figure 2), which matches the prediction from the parametric study by Williamson [31].

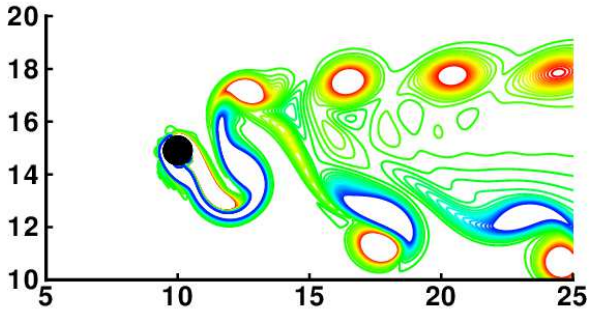

Figure 2. A snapshot at $T = 5$ from direct numerical simulation: vorticity is marked by contours.

Global POD modes were then computed from 400 snapshots of above simulation data which covers 4 time periods of the oscillation. It has been shown in our previous work [23], which using continuous solid domain integration (7–9), that the first 8 most energetic modes capture more than 90% energy and they are enough to capture basic dynamics. Here, to remove the computational cost burdened by the integration at each time steps, we will compare the results with the one using domain decomposition which has much lower time cost.

For solid decomposition, we also used 8 solid domain modes, which can describe the solid motion fairly well as shown in figure 3. The level-set equation (21) for solid domain change also shows an accurate estimation, as it is shown in the comparison of the phase portraits of coefficients computed by (21) and the exact solution directly from the POD of solid domain (figure 4).

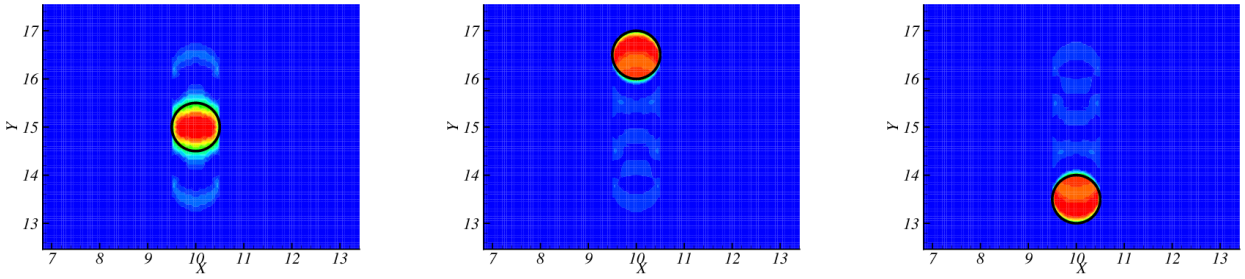

Figure 3. Comparison of the exact shape and location of the solid (black circle) and the shape rebuilt form 8 solid modes (color contours) at three time moments in one period: (a) $t = 0$, (b) $t = 1/4T$, (c) $t = 3/4T$.

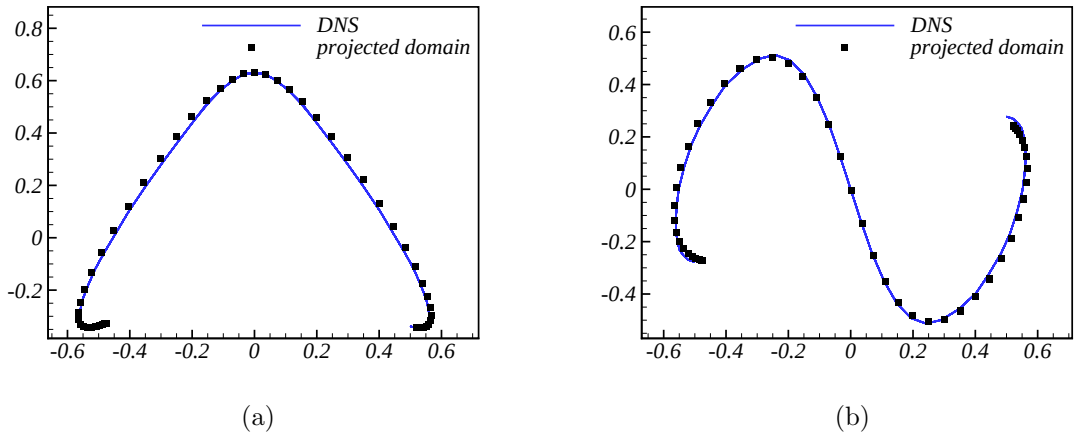

Figure 4. Phase portraits of the coefficients for solid domain modes: (a) (b_1, b_2) and (b) (b_1, b_3)

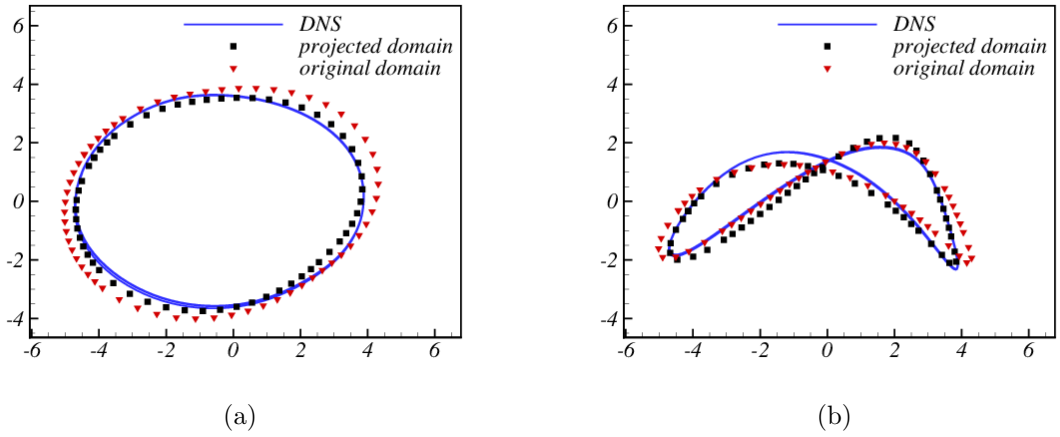

Figure 5. Comparison of phase portraits of global POD coefficients computed by DNS, solid domain decomposition (i.e. projected domain), and continuous solid domain (i.e. original domain): (a) (a_1, a_2) and (b) (a_1, a_3)

Finally, the overall results, shown by the phase portraits of global POD (for the combination of fluid and solid) coefficients, have also shown that the accuracy keeps almost the same in its comparison to the DNS

and the old ROM with continuous solid domain (figure 5).

III.B. Three-dimensional flow passing an oscillatory sphere

Similarly, the approach has been applied to a three-dimensional flow passing an oscillatory sphere. The Reynolds number defined by the sphere diameter and incoming velocity is 300. The computational domain is $l_x \times l_y \times l_z = (-2, 8) \times (-4, 4) \times (-2, 2)$ with uniform mesh at $N_x \times N_y \times N_z = 200 \times 160 \times 80$, and the neutral position of the sphere center is at $(x_0, y_0, z_0) = (0, 0, 0)$. The oscillation is defined by $y(t) = y_0 + A\sin(2\pi f t)$ with amplitude $A = 1.0$ and frequency $f = 0.16$. Figure 6 shows a typical snapshot from direct numerical simulation where vortex structures are shedding behind the sphere.

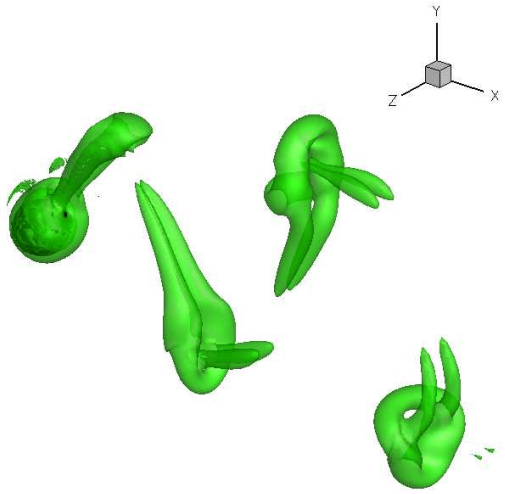

Figure 6. A typical snapshot from direct numerical simulation: vorticity structure of a flow passing an oscillatory sphere.

We first compare the accuracy of domain decomposition itself. Shown in figure 7, using 8 solid domain modes, we can capture the shape and location of solid domain (i.e. the sphere) in a very accurate manner.

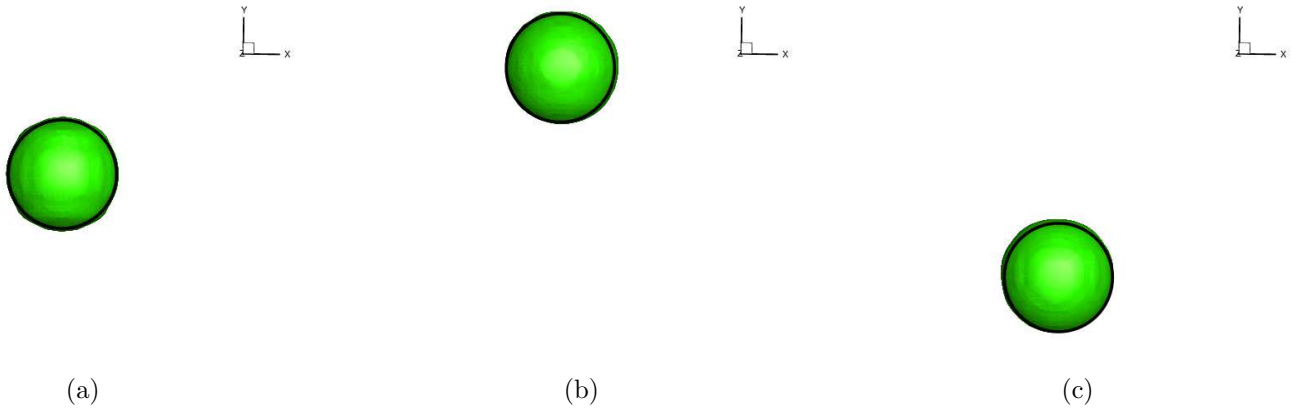

(a) (b) (c)

Figure 7. Comparison of the exact shape and location of the solid (black circle) and the shape rebuilt form 8 solid modes (iso-surface in green) at three time moments in one period: (a) $t = 0$, (b) $t = 1/4T$, (c) $t = 3/4T$.

The dynamics of the solid POD modes described by (21) and the global POD modes described by (18) has been captured successfully by the respective ROMs in a similar comparison of phase portraits of coefficients (figure 8 and 9).

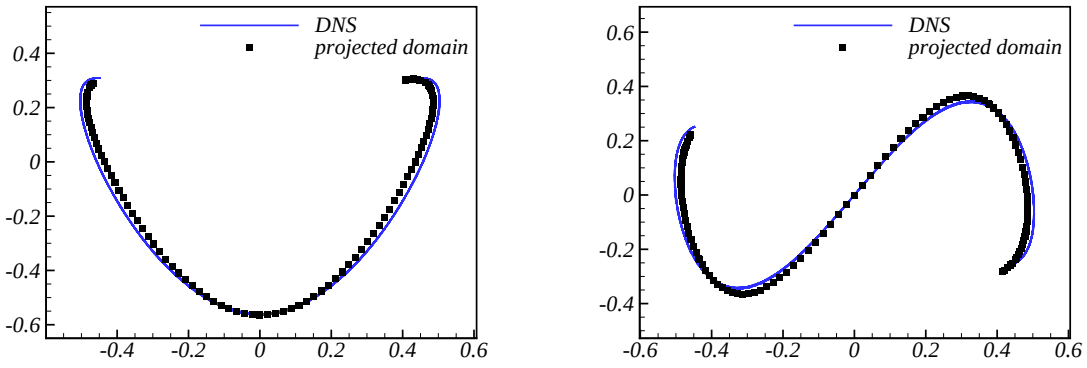

Figure 8. Phase portraits of the coefficients for solid domain modes: (a) (b_1, b_2) and (b) (b_1, b_3)

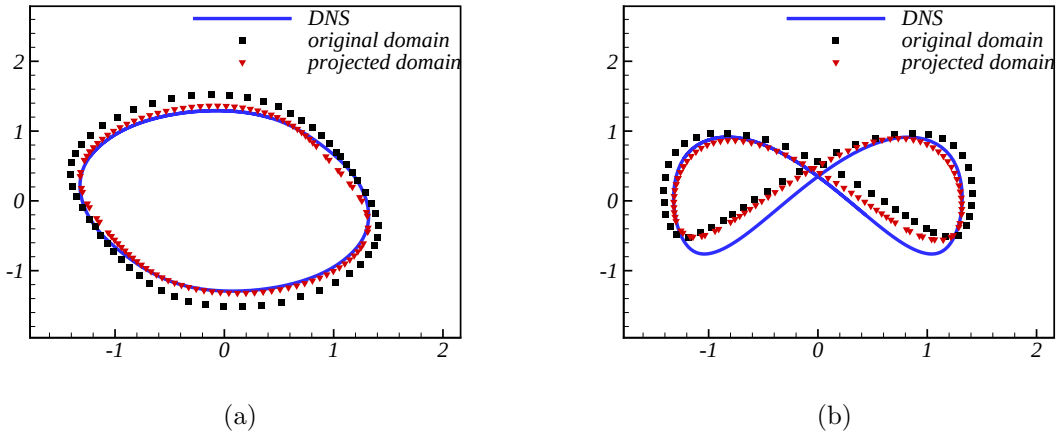

Figure 9. Comparison of phase portraits of global POD coefficients computed by DNS, solid domain decomposition (i.e. projected domain), and continuous solid domain (i.e. original domain): (a) (a_1, a_2) and (b) (a_1, a_3)

IV. Computational time cost for individual terms

In this section, analysis is taken to check the time cost of individual terms in the model (6) and seek the possibility of dropping expensive terms without sacrifice accuracy. For simplicity, terms are grouped and represent the model in a new form,

$$\dot{a}_i = F_i(a_j, a_k) + f_i^{(1)} + f_i^{(2)} + f_i^{(3)}. \tag{23}$$

The first term at the right-hand side,

$$F_i(a_j, a_k) = \frac{1}{\mathrm{Re}} \sum_{j=0}^{N} l_{ij} a_j + \sum_{j=0}^{N} \sum_{k=0}^{N} q_{ijk} a_j a_k, \tag{24}$$

is the same as the one existed in the traditional POD-Galerkin approach for fixed domain. Its coefficients stay fixed constants for both continuous and discrete domain-decomposition approaches. The other three terms, $f_i^{(s)}, s = 1, 2, 3$, represent the unsteady solid motion, and are defined differently in continuous and

domain-decomposition approaches. In continuous domain approach, they are

$$f_i^{(1)} = -\sum_{j=0}^{N} l'_{ij} a_j, \tag{25}$$

$$f_i^{(2)} = \sum_{j=0}^{N}\sum_{k=0}^{N} q'_{ijk} a_j a_k, \tag{26}$$

$$f_i^{(3)} = c'_i. \tag{27}$$

They need to be pre-computed for periodic prescribed motion or computed on-line at each step for more general situation. In discrete domain-decomposition approach, the solid terms are changed to

$$f_i^{*(1)} = -\sum_{j=0}^{N}\sum_{m=0}^{M} l^*_{ijm} b_m a_j, \tag{28}$$

$$f_i^{*(2)} = \sum_{j=0}^{N}\sum_{k=0}^{N}\sum_{m=0}^{M} q^*_{ijkm} b_m a_j a_k, \tag{29}$$

$$f_i^{*(3)} = \sum_{m=0}^{M} c^*_{im} b_m, \tag{30}$$

which have much lower time cost but still have room for improvement.

For better explanation, table 1 is introduced first to define basic numbers and typical time costs. It is noted that the cost estimations are all based on the current 2D and 3D cases, and adjustment is needed accordingly for other cases.

	Definition	Order estimation (2D/3D)
N	Number of fluid POD modes	10^1
M	Number of solid POD modes	10^1
N_p	Number of snapshots in one period	10^2
I	The inner product cost in the whole domain	$10^5H/10^6H$
I_s	The inner product cost in the neighborhood around the solid	$10^4H/10^5H$

Table 1. The definition and approximate cost of characteristic numbers and computational processes. H is used to indicate a computational time unit for a basic operation in integration.

Then, the cost of individual terms in (23) are estimated in table 2.

	Most time-costly computation	Time cost	Total order estimation (2D/3D)
$F_i(a_j, a_k)$	The inner product for q_{ijk}	$N^3 \times I$	$10^8H/10^9H$
$f_i^{(1)}$	The inner product for l'_{ij}	$N^2 \times I_s \times N_p$	$10^8H/10^9H$
$f_i^{(2)}$	The inner product for q'_{ijk}	$N^3 \times I_s \times N_p$	$10^9H/10^{10}H$
$f_i^{(3)}$	The inner product for c'_i	$N \times I_s \times N_p$	$10^7H/10^8H$
$f_i^{*(1)}$	The inner product for l^*_{ijm}	$N^2 \times I_s \times M$	$10^7H/10^8H$
$f_i^{*(2)}$	The inner product for q^*_{ijkm}	$N^3 \times I_s \times M$	$10^8H/10^9H$
$f_i^{*(3)}$	The inner product for c^*_{im}	$N \times I_s \times M$	$10^6H/10^7H$

Table 2. The time cost analysis for individual terms in ROM.

It is obvious that the nonlinear term for solid motion, $f_i^{(2)}/f_i^{*(2)}$, is the most expensive term for both continuous and domain-decomposition approaches. The next step is to plot the contribution of each terms in dynamics. figure 10 and figure 11 show respectively the contribution of these terms for the models using continuous and domain decomposition approaches.

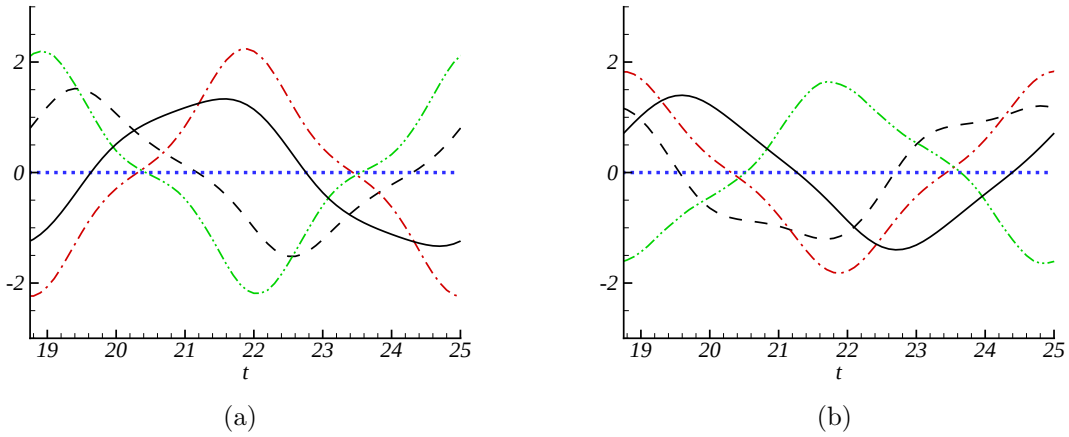

Figure 10. Contributions of each terms for the dynamics of the first two modes, (a) a_1 and (b)a_2, with solid domain being continuous: $(- - -)$ $F_i(a_j, a_k)$, $(- \cdot -)f_i^{(1)}$, $(\cdots)f_i^{(2)}$, $(- \cdot\cdot)f_i^{(3)}$, and $(\_\_\_)$ a_i

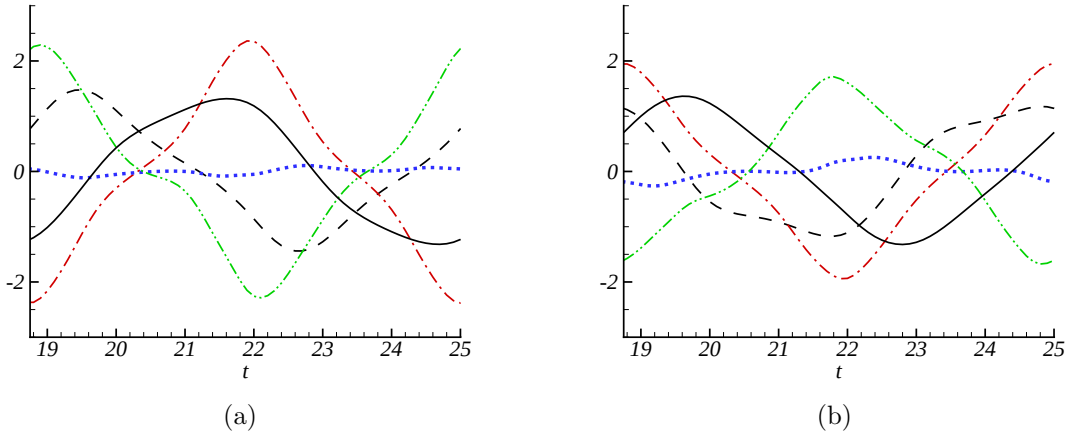

Figure 11. Contributions of each terms for the dynamics of the first two modes, (a) a_1 and (b)a_2, with domain decomposition of solid motion: $(- - -)$ $F_i(a_j, a_k)$, $(- \cdot -)f_i^{*(1)}$, $(\cdots)f_i^{*(2)}$, $(- \cdot\cdot)f_i^{*(3)}$, and $(\_\_\_)$ a_i

In both cases, the contribution of $f_i^{(2)}/f_i^{*(2)}$ is very small. To confirm its small impact to actual dynamics, we removed these nonlinear solid terms from the models and check the dynamics by the modified models. Figure 12 shows that almost the same accuracy is achieved by both continuous and domain-decomposition approaches when the expensive term is removed. As we noticed earlier in the table for cost comparison, the modified models have reduced the total cost by one order and make the on-line real-time computation possible.

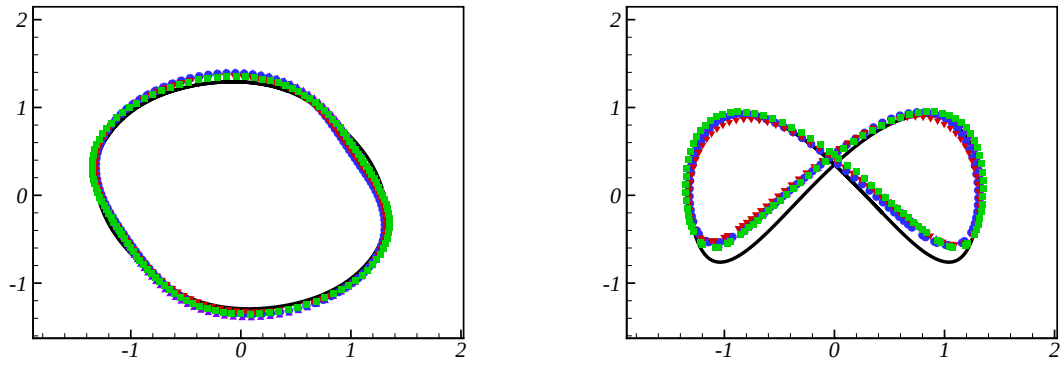

Figure 12. Phase portraits for the dynamics of the first two modes, (a) a_1 and (b) a_2: (——) DNS projection, (■) continues ROM with$f_i^{(2)}$, (▲) continues ROM without $f_i^{(2)}$, (●) decomposed ROM with $f_i^{*(2)}$, and (▼) decomposed ROM without $f_i^{*(2)}$

V. Conclusion

A global approach for model order reduction is developed for fluid dynamic problems with moving solid boundaries. Based on our earlier work using a continuous description of solid motion, we extended the work to consider the domain as decoupled modes. The domain decomposition approaches largely decreases the online time cost and make it possible to bring the entire computation of time-dependent coefficients on line while keeping a fast model for real-time applications. The model using domain decomposition shows reasonable accuracy in both solid location and fluid dynamics. We also noticed that the most expensive terms for both continuous and discrete domain approaches are the nonlinear solid terms and their contribution is actually negligible. The modified model without the expensive solid term shows almost the same accuracy as the complete model. This modification works for both continuous and decomposed domain approaches. All the results suggest the possibility of build a modified model with similar accuracy and much smaller computational cost.

Acknowledgment

The authors gratefully acknowledge the support from Army Research Laboratory through Micro Autonomous System and Technology (MAST) CTA and Army High Performance Computing Research Center (AHPCRC). HG would also thank the support by Graduate Research Enhancement Grant (GREG) of NMSU.

References

[1]Berkooz, G., Holmes, P., and Lumley, J. L., "The proper orthogonal decomposition in the analysis of turbulent flows," *Ann. Rev. Fluid Mech.*, Vol. 25, 1993, pp. 539–575.

[2]Holmes, P., Lumley, J. L., and Berkooz, G., *Turbulence, Coherent Structures, Dynamical Systems and Symmetry*, Cambridge University Press, Cambridge, 1996.

[3]Noack, B. R., Afanasiev, K., Morzynski, M., Tadmor, G., and Thiele, F., "A hierarchy of low-dimensional models for the transient and post-transient cylinder wake," *Journal of Fluid Mechanics*, Vol. 497, No. 1, 2003, pp. 335–363.

[4]Ma, X. and Karniadakis, G. E., "A low-dimensional model for simulating three-dimensional cylinder flow," *Journal of Fluid Mechanics*, Vol. 458, No. 1, 2002, pp. 181–190.

[5]Buffoni, M., Camarri, S., Iollo, A., Salvetti, M. V., et al., "Low-dimensional modelling of a confined three-dimensional wake flow," *Journal of Fluid Mechanics*, Vol. 569, 2006, pp. 141–150.

[6]Lieu, T. and Farhat, C., "Adaptation of aeroelastic reduced-order models and application to an F-16 configuration," *AIAA J.*, Vol. 45, No. 6, 2007, pp. 1244–1257.

[7]Siegel, S. G., Seidel, J., Fagley, C., Luchtenburg, D., Cohen, K., and McLaughlin, T., "Low-dimensional modelling of a transient cylinder wake using double proper orthogonal decomposition," *Journal of Fluid Mechanics*, Vol. 610, No. 1, 2008,

pp. 1–42.

[8]Wei, M. and Rowley, C. W., "Low-dimensional models of a temporally evolving free shear layer," *J. Fluid Mech.*, Vol. 618, 2009, pp. 113–134.

[9]Rowley, C. W. and Marsden, J. E., "Reconstruction Equations and the Karhunen-Loève Expansion for Systems with Symmetry," *Phys. D*, Vol. 142, 2000, pp. 1–19.

[10]Rowley, C. W., Colonius, T., and Murray, R. M., "Model reduction for compressible flow using POD and Galerkin projection," *Phys. D*, Vol. 189, No. 1–2, Feb. 2004, pp. 115–129.

[11]Noack, B. R., Schlegel, M., Morzyński, M., and Tadmor, G., "System reduction strategy for Galerkin models of fluid flows," *International Journal for Numerical Methods in Fluids*, Vol. 63, No. 2, 2010, pp. 231–248.

[12]Wei, M., Qawasmeh, B. R., Barone, M., van Bloemen Waanders, B. G., and Zhou, L., "Low-dimensional model of spatial shear layers," *Physics of Fluids*, Vol. 24, No. 1, 2012, pp. 014108.

[13]Cammilleri, A., Guéniat, F., Carlier, J., Pastur, L., Memin, E., Lusseyran, F., and Artana, G., "POD-spectral decomposition for fluid flow analysis and model reduction," *Theoretical and Computational Fluid Dynamics*, 2013, pp. 1–29.

[14]Tadmor, G., Lehmann, O., Noack, B. R., and Morzyński, M., "Galerkin models enhancements for flow control," *Reduced-Order Modelling for Flow Control*, Springer, 2011, pp. 151–252.

[15]Noack, B. R., Tadmor, G., and Morzynski, M., "Actuation models and dissipative control in empirical Galerkin models of fluid flows," *American Control Conference, 2004. Proceedings of the 2004*, Vol. 6, IEEE, 2004, pp. 5722–5727.

[16]Tadmor, G. and Noack, B. R., "Dynamic estimation for reduced Galerkin models of fluid flows," *American Control Conference, 2004. Proceedings of the 2004*, Vol. 1, IEEE, 2004, pp. 746–751.

[17]Anttonen, J., King, P., and Beran, P., "POD-based reduced-order models with deforming grids," *Mathematical and computer modelling*, Vol. 38, No. 1, 2003, pp. 41–62.

[18]Anttonen, J., King, P., and Beran, P., "Applications of multi-POD to a pitching and plunging airfoil," *Mathematical and computer modelling*, Vol. 42, No. 3, 2005, pp. 245–259.

[19]Feng, Z. and Soulaimani, A., "Nonlinear aeroelasticity modeling using a reduced order model based on proper orthogonal decomposition," *ASME Pressure Vessels and Piping Division Conference*, No. 26006, 2007.

[20]Liberge, E., Benaouicha, M., and Hamdouni, A., "Proper orthogonal decomposition investigation in fluid structure interaction," *European Journal of Computational Mechanics/Revue Européenne de Mécanique Numérique*, Vol. 16, No. 3-4, 2007, pp. 401–418.

[21]Liberge, E. and Hamdouni, A., "Reduced order modelling method via proper orthogonal decomposition (POD) for flow around an oscillating cylinder," *Journal of Fluids and Structures*, Vol. 26, No. 2, 2010, pp. 292–311.

[22]Wei, M. and Yang, T., "A global approach for reduced-order models of flapping flexible wings," AIAA paper 2010-5085, Chicago, IL, 2010.

[23]Gao, H. and Wei, M., "Global model reduction for flows with moving boundary," *AIAA Paper 2014-0222*, 2014.

[24]Peskin, C. S., "Flow patterns around heart valves: a numerical method," *J. Comput. Phys.*, Vol. 10, No. 2, 1972, pp. 252–271.

[25]Peskin, C. S., "Numerical analysis of blood flow in the heart," *J. Comput. Phys.*, Vol. 25, No. 3, 1977, pp. 220–252.

[26]Mohd-Yusof, J., "Combined immersed-boundary/B-spline methods for simulations of flow in complex geometries," Center for Turbulence Research, Annual Research Briefs – 1997, 1997.

[27]Zhao, H., Freund, J. B., and Moser, R. D., "A fixed-mesh method for incompressible flow-structure systems with finite solid deformations," *J. Comput. Phys.*, Vol. 227, 2008, pp. 3114–3140.

[28]Yang, T., Wei, M., and Zhao, H., "Numerical study of flexible flapping wing propulsion," 48th AIAA Aerospace Sciences Meeting and Exhibit, Orlando, FL, AIAA paper 2010-0553, 2010.

[29]Xu, M., Wei, M., Yang, T., Lee, Y. S., and Burton, T. D., "Nonlinear Structural Response in Flexible Flapping Wings with Different Density Ratio," 49th AIAA Aerospace Sciences Meeting and Exhibit, Orlando, FL, AIAA paper 2011-376, 2011.

[30]Brown, D. L., Cortez, R., and Minion, M. L., "Accurate projection methods for the incompressible Navier-Stokes equations," *J. Comput. Phys.*, Vol. 168, 2001, pp. 464–499.

[31]Williamson, C., "Vortex dynamics in the cylinder wake," *Annual review of fluid mechanics*, Vol. 28, No. 1, 1996, pp. 477–539.